CORRELATION OF GRAVIMETRIC AND SATELLITE GEODETIC DATA

Interim Progress Report Part I

Covering Period

September 11, 1967 – February 29, 1968

Prepared by

Gerald Ouellette
Pasquale Sconzo

Under

Contract NAS 12-598

for

National Aeronautics and Space Administration
Electronics Research Center
Cambridge, Massachusetts

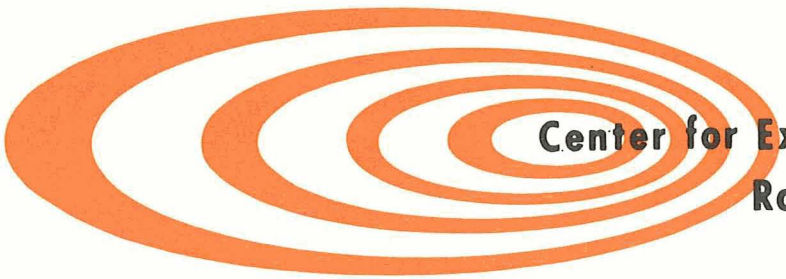

Center for Exploratory Studies
Rockville, Maryland

IBM

Correlation of Gravimetric and Satellite Geodetic Data

Prepared by

Cambridge Advanced Space Systems Department
International Business Machines Corporation
1730 Cambridge Street
Cambridge, Massachusetts

Contract Number NAS 12 - 598

Interim Scientific Report
Part I

Covering Period September 11, 1967 - February 29, 1968

Prepared for

Space Systems Group
National Aeronautics and Space Administration
Electronics Research Center
545 Technology Square
Cambridge, Massachusetts

Prepared by

Gerald A. Ouellette and Pasquale Sconzo

- TABLE OF CONTENTS -

		PAGE
1.	INTRODUCTION	
1.1	Scope of Work	1
1.2	Statement of the Problem	3
1.3	Philosophy of the Approach	4
2.	TECHNICAL APPROACH	
2.1	General Outline	5
2.2	The Geopotential Parameters and Their Associated Errors	7
2.3	Numerical Evaluation of the Positional Uncertainty	14
2.4	Data Generation and Plotting Routines	17
3.	ANALYSIS OF THE RESULTS	
3.1	General Discussion	19
3.2	Analysis of Computational Results	24
4.	FUTURE EFFORT	42
5.	REFERENCES	44
APPENDIX A.	The Earth's Geopotential	45
APPENDIX B.	Graphical Results (Bound Separately)	

1. INTRODUCTION

1.1 Scope of Work

Under Contract NAS 12-598, a study was carried out to ascertain the prediction accuracy in the position of a satellite over a 12-hr period at orbital altitudes where the period is approximately 100 minutes. The primary interest in this study was the effect of errors in the geopotential coefficients in position prediction. The study was to be definitive in that all procedures and assumptions were to be thoroughly checked so that all results could be trusted to be accurate. With this in mind, a base orbit was selected and analyzed extensively. The results of this analysis are now being extended to other orbits of interest.

The results obtained to date indicate that the position of a satellite in a nearly circular orbit, inclined 45°, with a period of about 100 minutes can be predicted to within $\pm$ 10 meters over a 12-hr period if a correlated set of geopotential coefficients is used. In particular, a set complete through $n = m = 8$ with a few specific terms beyond 8 is sufficient to obtain this accuracy.

A numerical integration program was utilized to determine the error growth in position prediction by comparing a perturbed orbit with a nominal reference orbit. Since each harmonic coefficient was perturbed independently, the superposition of coefficient errors was analyzed to examine the validity of this approach. The results of this analysis proved that, for the current effort, all the errors sum linearly to produce the composite or total error.

Unusual or unanticipated results in the numerical procedure were investigated analytically to determine the theoretical reasons for the behavior. One of these, the secular growth of in-track error, is discussed in Section 3.2. Also, the accuracy of the various published coefficient models was investigated to provide a quantitative measure of comparison

between various results obtained in coefficient determination and is discussed in Section 2.2. The necessity for a well correlated coefficient matrix is discussed in various sections.

Technical sections of this report include a statement of the problem, the philosophy of the approach, preliminary results, and suggestions for further effort. Graphical results are presented in Appendix B.

1.2 Statement of the Problem

The current literature contains many articles, papers and comments concerning the prediction accuracy attainable with various models for the forces acting on a satellite. Of these forces, the one produced by the gravitation field of the earth seems to be the center of much controversy. The current practice is to represent the gravitational potential by a truncated series of Legendre polynomials with harmonic coefficients. A pertinent question is, how many terms are required and how accurately must they be known to predict satellite position to within $\pm$ 10 meters of its true position for a period of up to twelve hours using satellites in near circular orbits with periods on the order of 100 minutes.

On looking into the literature it becomes readily apparent that there is no agreement as to what is required to answer this question. The variance between authors in terms of prediction accuracy for similar models ranges up to three orders of magnitude. To answer the question, therefore, it was decided that a complete andunified analysis of the error propagation was needed and was therefore initiated. This document provides a partial answer and lays the groundwork for further effort to produce a complete answer within the constraints of the question.

1.3 Philosophy of the Approach

As discussed in the statement of the problem, there are conflicting views on the requirements of a geopotential model suitable for precision prediction of satellite motion. There is even some question on the definition of precision prediction since requirements vary for different missions. For the current study, therefore, an arbitrary figure of 10 meters in any direction is taken to be the value of a precision prediction. At a slant range of 1500 km, this represents an error of about 1".5 in position angle for an error perpendicular to the line of sight. The best photoreduced observations currently available from the Smithsonian Astrophysical Observatory have a standard deviation of about 4 seconds of arc. These are not used in precision prediction since there is a long time delay (weeks to months) in obtaining the reduced data, which is only useful in non-real time analysis.

Second and higher order effects in the geopotential create disturbances in the motion that are greater than 10 meters, hence analytic formulations were not utilized in the study computations, except where they were exact or could definitely be shown to cause no measurable error. Numerical integration techniques were used to generate the nominal prediction ephemeris and the various perturbed trajectories. The techniques were numerically tested to demonstrate that individually computed errors summed to the total error.

When it can be demonstrated that analytic approximations will provide sufficient accuracy for parameterizing results with respect to altitude, inclination, and nodal position, they will be introduced to provide greater generality and simplicity.

2. TECHNICAL APPROACH

2.1 General Outline

The procedure utilized in carrying out the error propagation study was to compare the position of a satellite moving in a reference trajectory with that of the same satellite moving along a perturbed trajectory at some specified time. The reference trajectory consisted of a satellite ephemeris generated under the gravitational influence of the zonal earth with zonal terms including $C_{2,0}$, $C_{3,0}$ and $C_{4,0}$. The geopotential coefficients through 14, 14 were then individually introduced with a multiplication factor to simulate an error in the coefficient. A numerical integration program was utilized to generate the ephemeris and the perturbed trajectory was compared with the reference trajectory at each time step. The differences between the position coordinates of the satellite were resolved through vector projection on to a satellite centered coordinate system as described in Section 2.3. This procedure provides the components of the error along three directions of interest. In fact, observing that the perturbed trajectory is a curve with two curvature radii, the first component of the error (in-track component) is taken along the satellite's velocity direction which is tangent to the trajectory. The second component is along the principal normal toward the center of the osculating circle to the trajectory. This second component may be called the normal cross-track error and of course it is normal to the first component. A third component forming a right-hand triad with the other two is taken in the direction of the bi-normal to the trajectory.

The three components of the position error associated with uncertainties or errors in the coefficients were plotted automatically as a function of time. The procedure for the plotting routines is outlined in Section 2.4. During the analysis, it was noted that the in-track components showed a definite secular trend when many of the coefficients were perturbed. This secular trend, described in Section 3.2 is due primarily to the slight change in the total energy resulting from the introduction of a coefficient without a compensating change in the initial conditions. This secular trend

disappears when all the coefficients are introduced and could provide a measure for the correlation of the various coefficients in a geopotential model. In discussing positional errors due to uncertainties in various harmonics, secular deviations are not considered. This is because these deviations may be accounted for by slight variations in the initial conditions which compensate for the energy change.

A discussion of the results and their validity is given in Section 3. Appendix B of the report contains a complete graphical presentation of the prediction error associated with the geopotential coefficients through 14, 14. A brief general discription of the geopotential is also included in Appendix A for the benefit of those who are unfamiliar with the standard notation.

2.2 The Geopotential Parameters and Their Associated Errors

We deem it necessary and also appropriate that a discussion about the statistical data concerning the geopotential parameters and their associated errors shall precede the analysis of their effect on satellite positions. There is a general feeling, although not enough and openly expressed, that the gravitational parameters appearing in the expressions for the geopotential – developed in terms of zonal, sectorial and tesseral harmonics – are poorly determined. How poor is this determination? We will aim at answering this question with the intent of giving supporting numerical evidence to the feeling mentioned above.

Let us take a look at the various determinations made by different investigators. The first fact arising from a preliminary inspection of the existing published determinations is that the values given by different investigators agree fairly well up to the second order model of the geopotential. But going to the third order model there is a patent disagreement which becomes worse for models of order greater than three. As an illustration of this situation we list below the discrepancies found in $\overline{C}_{n,m}$ and $\overline{S}_{n,m}$ (n = 3; m = 1, 2, 3) among the values given by Izsak (I), Guier and Newton (G), Anderle (A) and Rapp (R).

Coeff.	Value Given by I	Differences I-G	G-A	I-A	I-R
$\overline{C}_{31}$	1.60	-0.24	-0.31	-0.55	+0.49
$\overline{C}_{32}$	0.38	-0.84	+0.24	-0.60	-0.45
$\overline{C}_{33}$	-0.17	-0.83	+0.08	-0.75	-1.29
$\overline{S}_{31}$	-0.04	-0.25	-0.06	-0.31	+0.13
$\overline{S}_{32}$	-0.80	-0.12	+0.23	+0.11	-0.22
$\overline{S}_{33}$	1.40	+0.42	-0.64	-0.22	+0.28

The $\overline{C}_{n,m}$ and $\overline{S}_{n,m}$ are fully normalized coefficients. The values given are of the order 10^{-6}. For the source the reader is referred to Kaula (1966) and Rapp (1967).

No comments are needed on the contents of the above table because the values of the differences speak for themselves. It could be objected that these differences are partly due to the different techniques used (satellite optical and/or doppler data solely or in combination with gravimetric measurements). We think, however, that these differences arise from the intrinsic difficulty of separating small components from a small global effect which is ultimately the observable datum. By using satellites the situation is aggravated by the fact that the global effect observed upon their motion is intermingled with other small effects whose cause is not fully predictable and consequently not rigorously computable. The conclusion is that we are still not sure about the values of the coefficients constituting the third order model of the geopotential. Needless to say that this is also true for higher order models.

Sometimes one who wishes to use these parameters has no knowledge of the errors associated to them. In fact because of the difficulty in determining the errors, many investigators very often neglect publishing the standard error associated with each parameter so that it is impossible to arrive at a judgement about the accuracy of their determinations. This lamentable omission was not made in the referenced paper by Rapp, thus, our further discussion will be based on the contents of Table V, pp 14-15, of Rapp's paper. This table represents a combined solution of gravimetric and satellite data up to the parameters (14, 14). Inspecting the column of this table headed "Standard Error" one may immediately perceive that the value $\sigma_{n,m}$ of this error is too large and often greater than the absolute value of the magnitude of the corresponding coefficients. How often does this occur? Does it occur more frequently for high-order coefficients than for low-order coefficients ?

For answering these questions we define the quantity ρ as follows:

$$\rho = \frac{\sigma_{n,m}}{|J_{n,m}|}$$

where $J_{n,m}$ is either $\overline{C}_{n,m}$ or $\overline{S}_{n,m}$. Next we classify the potential coefficients in three categories (I), (II) and (III) according to

(I) $\rho \leq 0.25$

(II) $0.25 < \rho < 1$

(III) $\rho \geq 1$

Then, from the said Table V the following one can be derived

Categorization of the Geopotential Coefficients

Model		Category (I)	(II)	(III)	Totals
		Number of Coefficients			
from (3, 0) to (6, 6)	$C_{n,m}$	10	8	4	
	$S_{n,m}$	11	4	3	
		21	12	7	40
from (7, 0) to (8, 8)	$C_{n,m}$	2	11	4	
	$S_{n,m}$	2	9	4	
		4	20	8	32
from (9, 0) to (10, 10)	$C_{n,m}$	1	15	5	
	$S_{n,m}$	1	10	8	
		2	25	13	40
from (11, 0) to (12, 12)	$C_{n,m}$	2	13	10	
	$S_{n,m}$	0	11	12	
		2	24	22	48
from (13, 0) to (14, 14)	$C_{n,m}$	3	14	12	
	$S_{n,m}$	2	13	12	
		5	27	24	56

The grand totals and the corresponding % are:

Category (I)	(II)	(III)	Total
34	108	74	216
15.7%	50%	34.3%	

Now, according to common sense, the coefficients belonging to category (I) can be considered as fairly well determined. This group represents, however, a small percentage (15.7%) of the totality of the coefficients. In their majority these coefficients belong to the geopotential model up to (6, 6). Those coefficients belonging to category (II) should be considered as poorly determined coefficients. Their number initially increases by increasing the order of the model, then they level off at 50% of the totality. Finally, the coefficients belonging to category (III) should be considered as having no physical meaning and should, therefore, be considered as unknown. This last group represents a sizeable part of the totality. (34.3%)

All these findings indicate that the geopotential determination becomes of poor quality by increasing the order of the model. Figure 2 - 1 illustrates this graphically.

Classification of Geopotential Coefficients

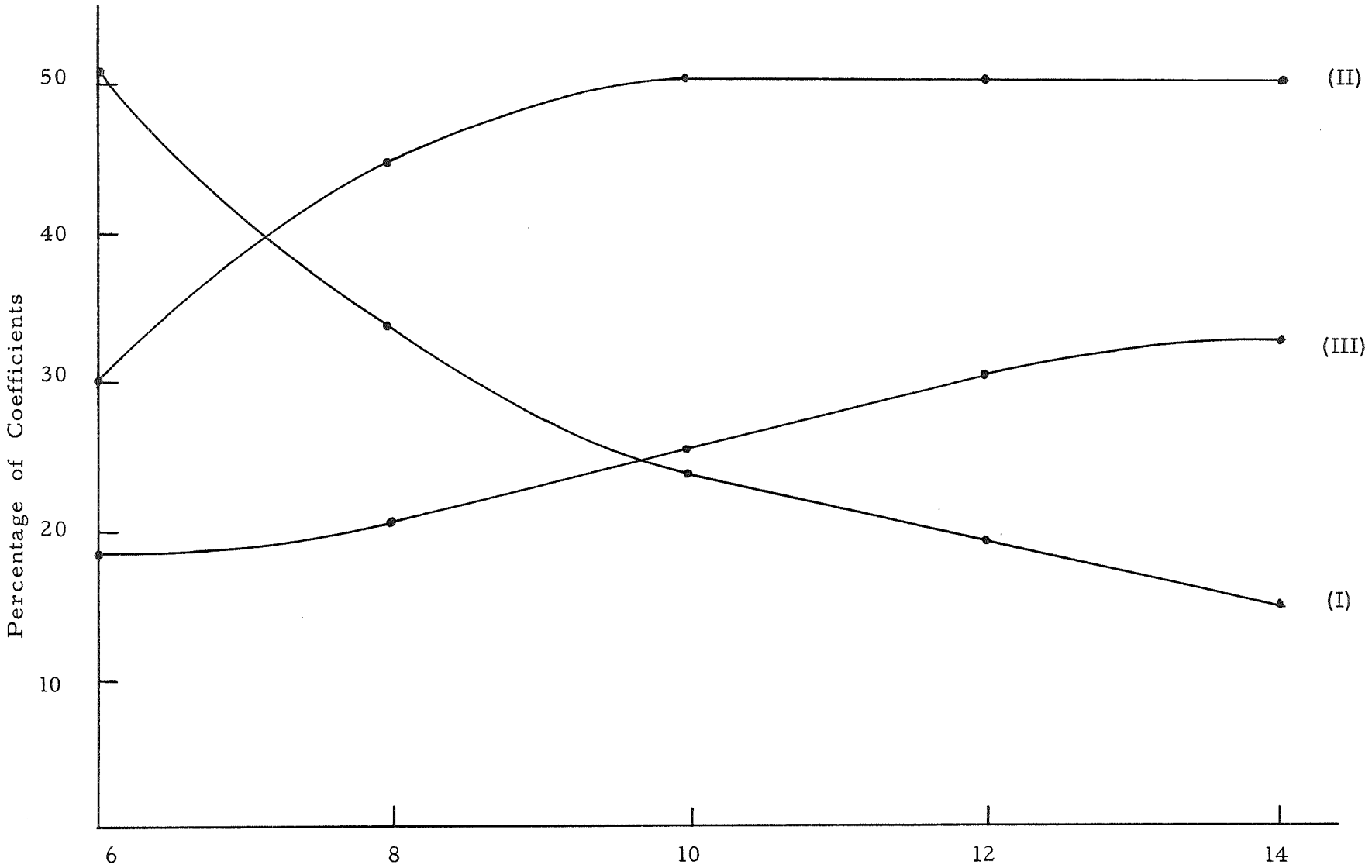

Figure 2-1

For the convenience of any user of Rapp's model we list here the 74 coefficients for which $\rho > 1$.

$C_{5,5}$ $C_{6,2}$ $C_{6,4}$ $C_{6,6}$

$S_{5,1}$ $S_{5,3}$ $S_{6,1}$

$C_{8,0}$ $C_{8,3}$ $\underline{C_{8,4}}$ $C_{8,7}$

$S_{7,1}$ $S_{7,3}$ $S_{7,4}$ $\underline{S_{8,1}}$

$C_{9,5}$ $C_{9,6}$ $C_{9,9}$ $C_{10,3}$ $C_{10,8}$

$S_{9,3}$ $S_{9,4}$ $S_{9,5}$ $S_{9,7}$ $S_{9,9}$ $S_{10,5}$ $S_{10,7}$ $S_{10,9}$

$C_{11,1}$ $C_{11,4}$ $C_{11,7}$ $C_{11,9}$ $C_{11,10}$ $\underline{C_{12,1}}$ $C_{12,4}$ $C_{12,5}$ $\underline{C_{12,10}}$ $C_{12,11}$

$S_{11,1}$ $S_{11,2}$ $S_{11,3}$ $S_{11,6}$ $S_{11,9}$ $S_{11,10}$ $S_{11,11}$ $S_{12,3}$ $S_{12,4}$ $S_{12,6}$ $S_{12,10}$ $S_{12,11}$

$C_{13,2}$ $C_{13,3}$ $C_{13,4}$ $\underline{C_{13,7}}$ $C_{13,9}$ $C_{13,10}$ $C_{13,12}$ $C_{13,13}$ $C_{14,0}$ $C_{14,1}$ $C_{14,8}$ $C_{14,13}$

$S_{13,2}$ $S_{13,7}$ $\underline{S_{13,8}}$ $\underline{S_{13,11}}$ $S_{14,1}$ $S_{14,2}$ $\underline{S_{14,3}}$ $S_{14,4}$ $S_{14,8}$ $S_{14,11}$ $\underline{S_{14,12}}$ $S_{14,14}$

The underlined coefficients correspond to $\rho >> 10$.

Having ascertained that the knowledge of the fine structure of the geopotential is far from being satisfactory, we may, however, say that Rapp's model, as well as the other models, are capable of representing fairly accurately the motion of a satellite during a certain period of time. This representation is a purely numerical fit of the observations to a pre-assigned model (which is not required, with the exception of a few resonant terms for the analysis of some particular orbits, to be of an excessively high order), but we must abstain from attributing physical meaning to the values of most of the $C_{n,m}$ and $S_{n,m}$ coefficients. The said fitting procedure between the observable and the model may be achieved if we do not care that, for this achievement, we must accept the existence of several

numerical correlations among the geopotential coefficients and the coordinates of the observing stations and the coefficients themselves. (See Izsak 1964). These correlations are, however, inexplicable and remain not clearly understood.

It may be of interest to notice that in regard to their sign the geopotential coefficients are distributed as follows

	Positive	Negative	
$C_{n,m}$	63	51	
$S_{n,m}$	42	60	
	105	111	216

The two groups are almost evenly populated. This confirms qualitatively that a sort of compensation of small opposite effects takes place and, hence, that the said fit may be achieved.

We remark also that the smallness of the global effect is a consequence of the fact that the coefficients themselves are small. In fact, excluding the 2nd order coefficient, all the other are distributed as follows

		Between	
	$> 10^{-7}$	10^{-8} and 10^{-7}	$< 10^{-8}$
$C_{n,m}$	22	73	19
$S_{n,m}$	22	61	19
	44 (20.4%)	134 (62%)	38 (17.6%)

Finally, we notice that all the coefficients $< 10^{-8}$ belong to category (III). An alternate approach to analyzing the errors in the coefficients has been taken by Strange, et al (1967) whereby he uses the errors associated with observations to arrive at error bounds on the coefficients.

2.3 Numerical Evaluation of the Positional Uncertainty

The positional uncertainties of the satellite are presented in the satellite centered coordinate system illustrated in Figure 2-2. The vector difference between satellite coordinates in a perturbed and unperturbed mode is projected upon the reference axes as a function of time. These projections provide a measure of the positional uncertainty growth with respect to the orbital motion. Thus, $\Delta\vec{r}(t)$ becomes $\Delta\vec{s}$, $\Delta\vec{b}$, $\Delta\vec{n}$ where

$\Delta\vec{s}$ is the in track error (colinear with the velocity vector)

$\Delta\vec{b}$ is the bi-normal error (perpendicular to the orbit plane)

$\Delta\vec{n}$ is the principal normal error (perpendicular to both $\Delta\vec{s}$ and $\Delta\vec{b}$).

By virtue of the additive property of small perturbations, the contribution caused by errors in the geopotential coefficients can be summed over the coefficients to determine their total contribution. Numerical procedures have been used to confirm this assumption.

The prediction uncertainty due to errors in the geopotential is obtained from the difference between satellite coordinates in an unperturbed orbit $(x, y, z, \dot{x}, \dot{y}, \dot{z})$ and the coordinates in a perturbed orbit $(x^*, y^*, z^*, \dot{x}^*, \dot{y}^*, \dot{z}^*)$. As we have said before, the unperturbed orbit utilizes a set of zonal coefficients through $C_{4,0}$, while the perturbed orbit utilizes this same set of coefficients, plus the coefficient of interest with an error factor. At specified time intervals, the perturbed orbit coordinates are compared with the reference orbit to provide a measure of $\Delta\vec{s}$, $\Delta\vec{b}$, $\Delta\vec{n}$ as follows,

$$\Delta s = (\vec{v} \cdot \Delta\vec{r})/v$$

$$\Delta b = \vec{L} \cdot \Delta\vec{r}/L$$

$$\Delta n = \vec{L} \times \vec{v} \cdot \Delta\vec{r}/v\,L$$

where

$$\vec{r} = x\hat{i} + y\hat{j} + z\hat{k}$$

$$\Delta\vec{r} = (x^* - x)\hat{i} + (y^* - y)\hat{j} + (z^* - z)\hat{k}$$

COORDINATE SYSTEM FOR REPRESENTING POSITIONAL UNCERTAINTIES

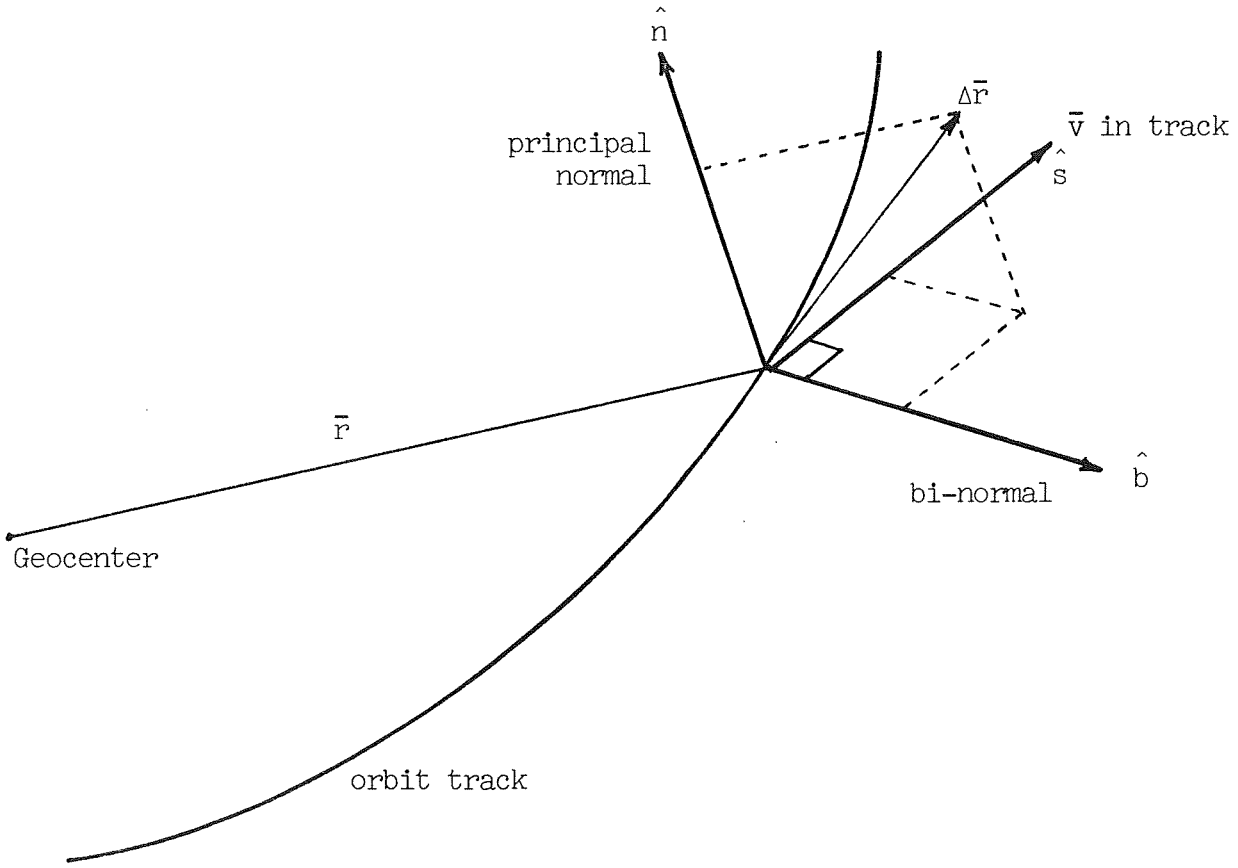

Components of Δr :

$$\Delta s = \frac{1}{v} (\dot{x}\Delta x + \dot{y}\Delta y + \dot{z}\Delta z)$$

$$\Delta n = \frac{1}{vL} (\lambda\Delta x + \mu\Delta y + \nu\Delta z)$$

$$\Delta b = \frac{1}{L} (C_x\Delta x + C_y\Delta y + C_z\Delta z)$$

where

$$\bar{r} \times \bar{v} = \hat{i}C_x + \hat{j}C_y + \hat{k}C_z$$

$$\sigma = \bar{r} \cdot \bar{v}$$

$$\bar{v}\sigma - \bar{r}v^2 = \lambda\hat{i} + \mu\hat{j} + \nu\hat{k}$$

$$L = \left| \bar{r} \times \bar{v} \right|$$

Figure 2 - 2

$$\vec{v} = \dot{x}\hat{i} + \dot{y}\hat{j} + \dot{z}\hat{k}$$

$$\vec{L} = \vec{r} \times \vec{v}.$$

The Δs, Δb, Δn values have been plotted as functions of time for a period of 900 minutes (see Sec. 3)

2.4 Data Generation and Plotting Routines

The data generation program utilized in these studies is a modified version of a satellite orbit and atmospheric density determination program developed for the Air Force Cambridge Research Laboratories under Contract Number F19628-68-C-0032. This program is particularly well suited for the current application since it includes a provision for introducing a geopotential model to any order in the prediction portion of the program. It is capable of generating ephemerides containing very little truncation and round off error. The accuracy of the data generation program has been verified by comparing results obtained from it with independently published results and by various closure tests which indicate a total error of about 1 meter in a 24 hour prediction.

The program presently runs on an IBM 7094 computer and uses a Runge - Kutta scheme to integrate the differential equations of motion represented in a geocentric inertial Cartesian coordinate system. At each integration step, the necessary transformations are made to determine the gravitational attractions due to selected zonal and tesseral terms, and the resulting trajectory is compared on a point by point basis with a nominal trajectory containing only zonal terms through $C_{4,0}$. Differences between the two trajectories at each time step are converted into a Cartesian coordinate system described in Section 2.3. These error components are stored for introduction into a plotting routine for generating graphical results.

The plotting routine is designed to operate in conjunction with a Cal Comp plotter. Labeling of graphs for identification purposes along with automatic scaling of abcissa and ordinate values is performed. The error component data is then plotted at sufficiently small time intervals to give the appearance of continuous curves without introducing excess clutter into the graphs.

At present the program is being modified to include a more efficient numerical integration procedure which will speed up the computations and which will maintain a higher degree of accuracy.

3. ANALYSIS OF THE RESULTS

3.1 General Discussion

This discussion is based on the results of a large number of numerical integrations (about 300) displayed in diagrams which have been plotted automatically. Most of these diagrams are collected in Appendix B.

We begin by observing that both the geopotential coefficients and their associated errors are small quantities. They are smaller than 10^{-7} in the majority. Thus, we can make use of the additive property of small perturbations and infer the effect of the uncertainty in a single term of the geopotential upon the position of a satellite from the effect induced by this term. It was expected that the first effect would be proportional to the second. The numerical analysis has confirmed this expectation. An illustration of this finding is given in Figures 3-1 and 3-2. The first shows the growth of the error induced by $C_{2,2}$. The second shows the same when $FC_{2,2}$ is used instead of $C_{2,2}$. The factor F has been chosen according to $FC_{2,2} = \sigma(C_{2,2})$. In this actual case, $F = 0.023235$. At the end of the same time interval the original in-track error ΔS reduces to the new in-track error $\overline{\Delta S}$, and it is $\overline{\Delta S} = F \Delta S = 80$ meters. A similar conclusion can be made comparing the graph for $S_{3,3}$ (Figure 3-3) with that of $FS_{3,3}$ (Figure 3-4) where $F = 0.048341$.

Here, we shall emphasize the special feature of our computer program which allows the handling of any uncertainty α associated with $J_{n,m}$ by means of a factor F such that $FJ_{n,m} = \alpha$. There is, in particular, a value of F such that $FJ_{n,m} = \sigma_{n,m}$ as it was the case of the examples reported above.

M	OMEGA	C OMEGA	I	E	A
0.0000	0.0000	0.0000	45.00000	.00500000	7136.6535

RUN FOR C(2 ,2) = 2.3241
FACTOR USED IS 1.000000

(*) IN-TRACK
(+) PRINCIPAL NORMAL CROSS-TRACK
(⊙) BI-NORMAL CROSS-TRACK

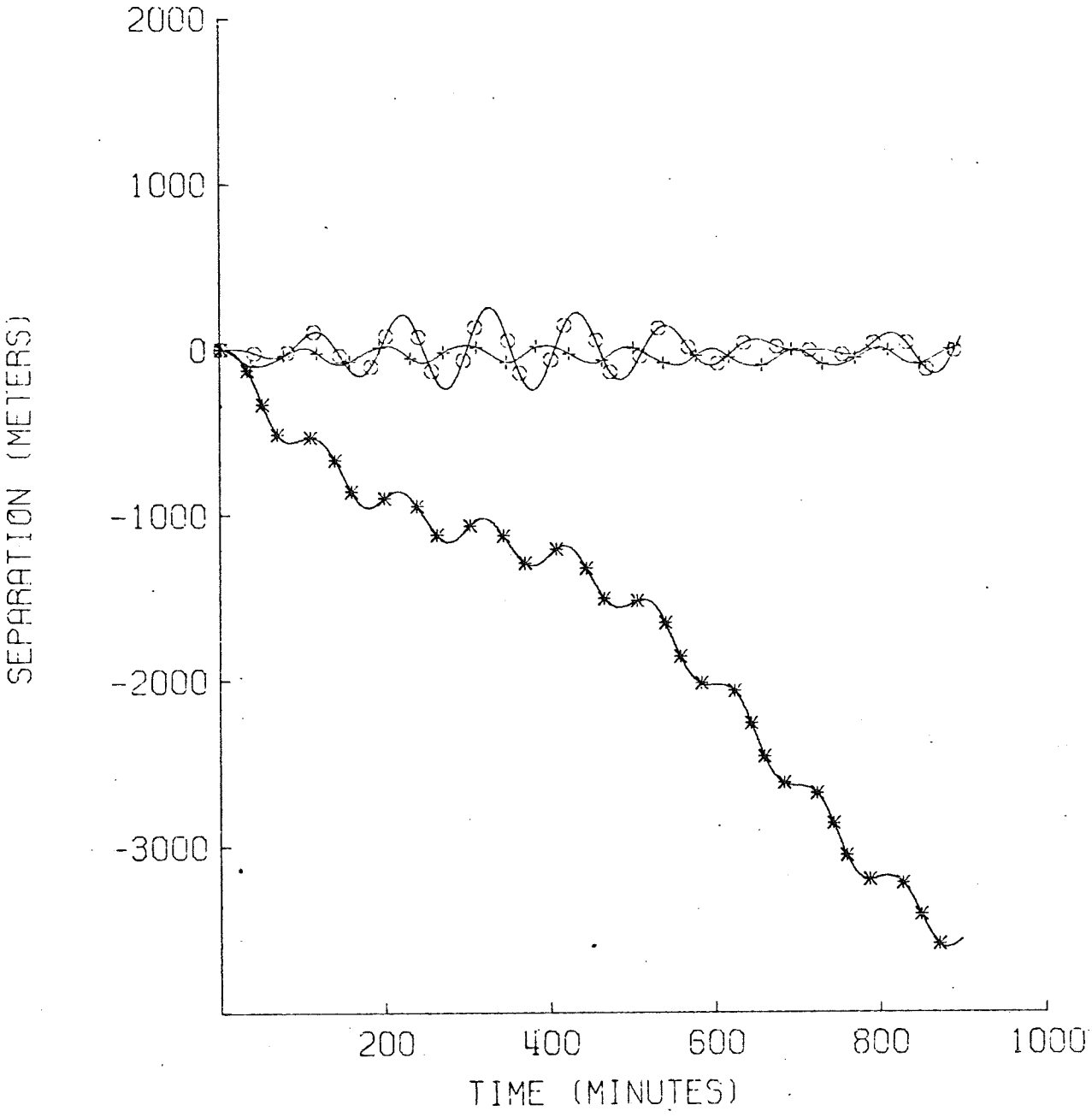

Figure 3 - 1

M	OMEGA	C OMEGA	I	E	A
0.0000	0.0000	0.0000	45.00000	.00500000	7136.6535

RUN FOR C(2 , 2) = 2.3241
FACTOR USED IS .023235

(*) IN-TRACK
(+) PRINCIPAL NORMAL CROSS-TRACK
(⊙) BI-NORMAL CROSS-TRACK

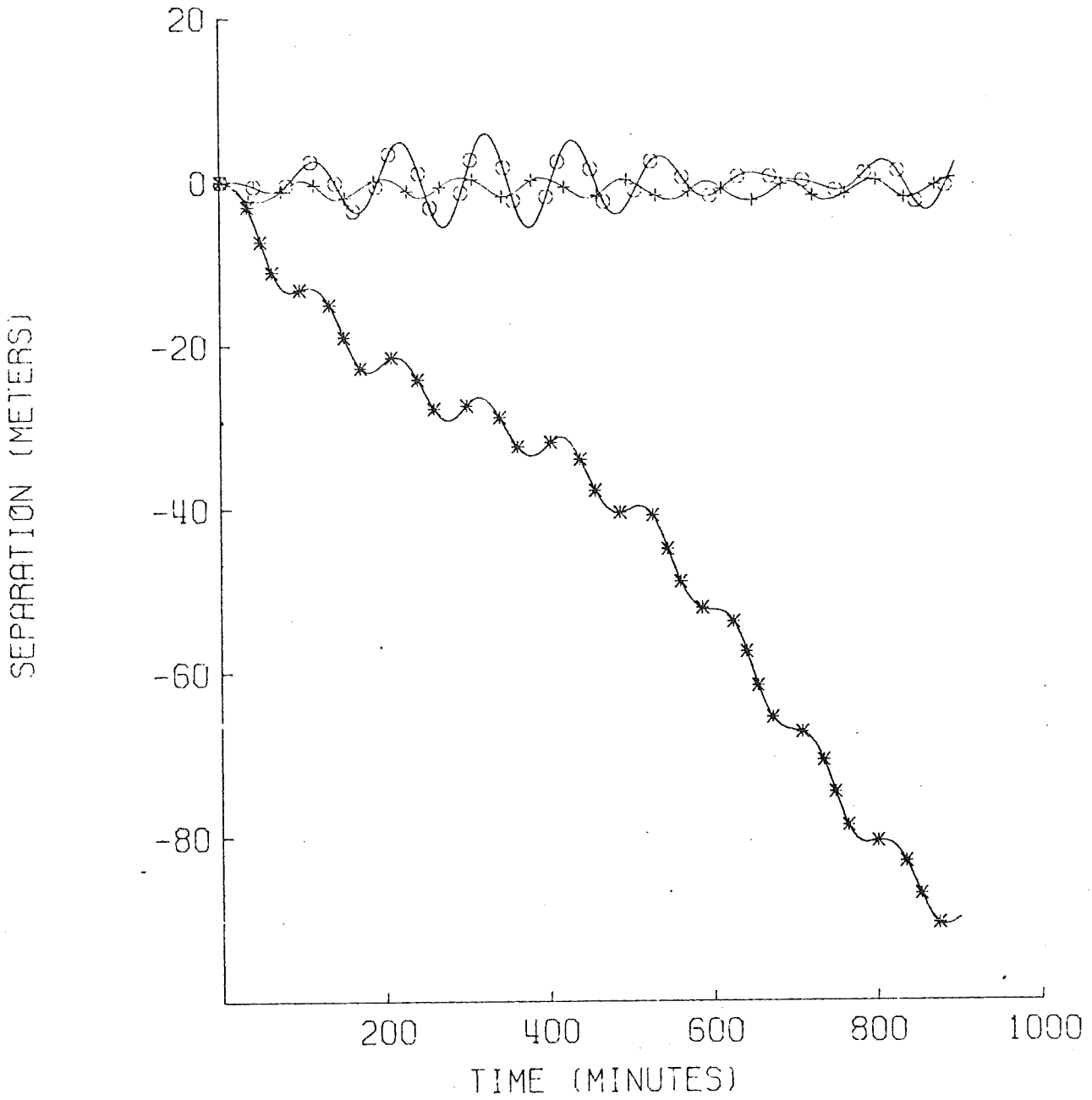

Figure 3-2

M	ØMEGA	C ØMEGA	I	E	A
0.0000	0.0000	0.0000	45.00000	.00500000	7136.6535

RUN FØR S(3 , 3) = 1.3860
FACTØR USED IS 1.000000

(*) IN-TRACK
(+) PRINCIPAL NØRMAL CRØSS-TRACK
(⊙) BI-NØRMAL CRØSS-TRACK

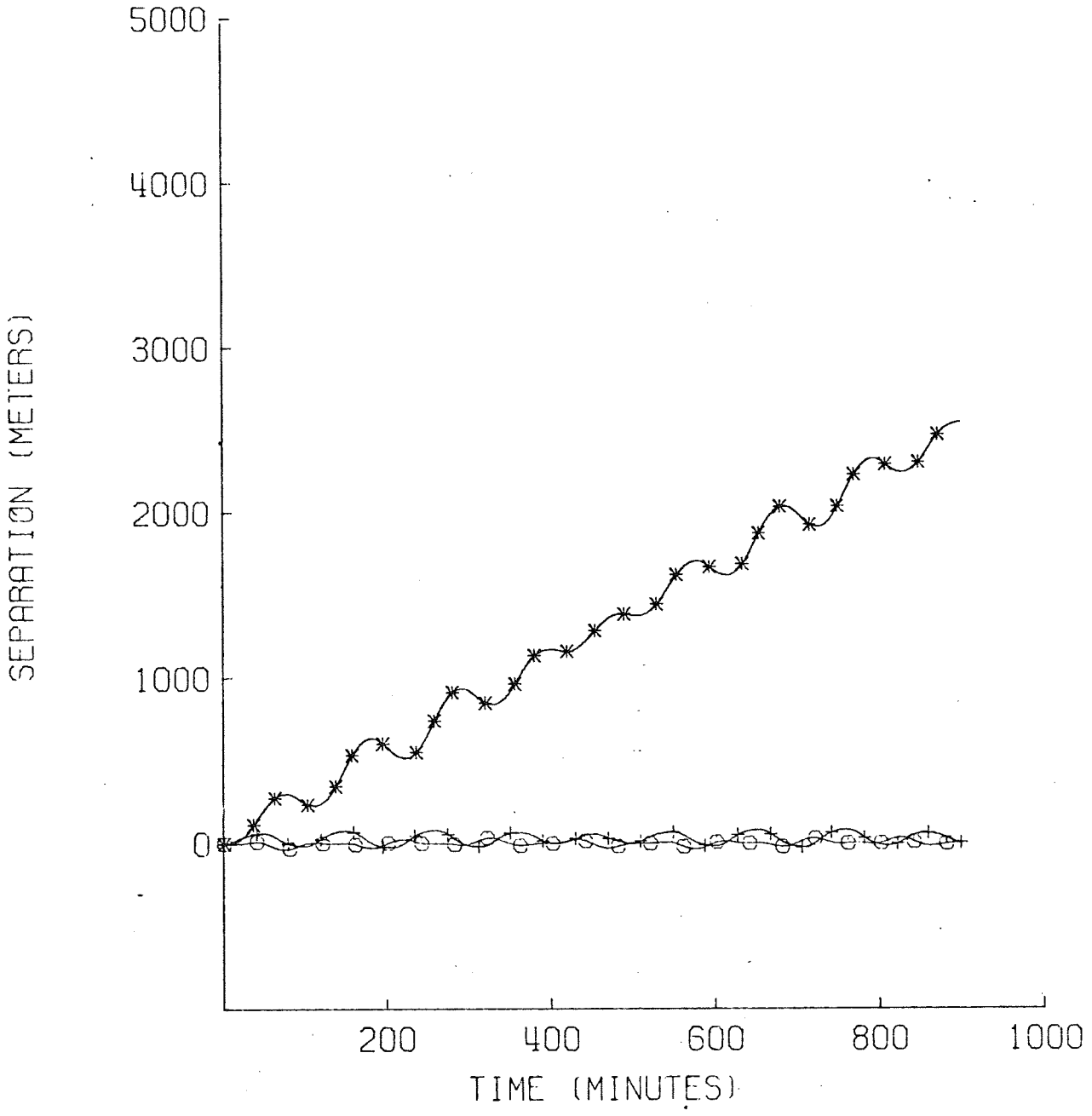

Figure 3 - 3

M	OMEGA	C OMEGA	I	E	A
0.0000	0.0000	0.0000	45.00000	.00500000	7136.6535

RUN FOR S(3 , 3) = 1.3860
FACTOR USED IS .048341

(*) IN-TRACK
(+) PRINCIPAL NORMAL CROSS-TRACK
(⊕) BI-NORMAL CROSS-TRACK

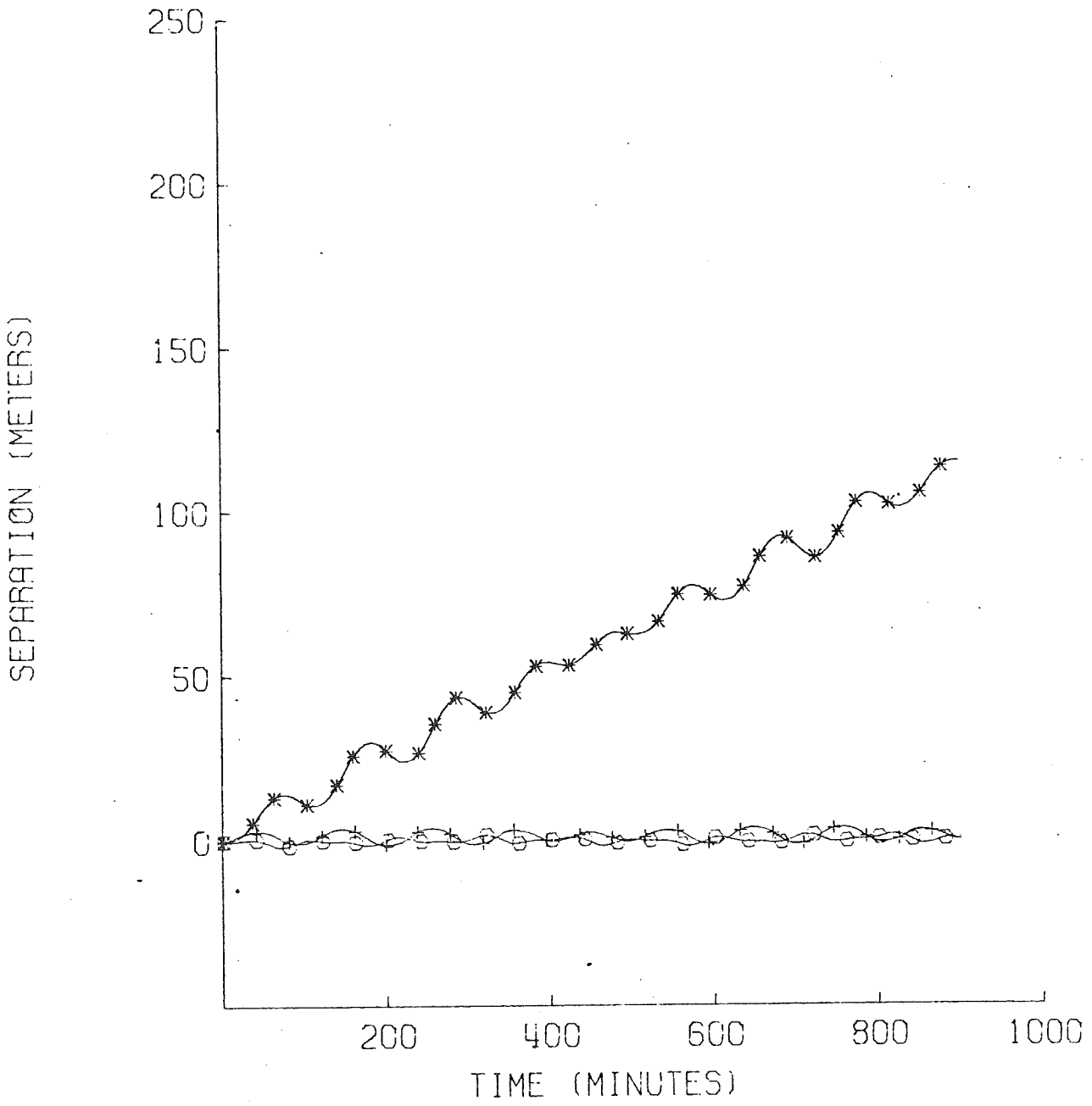

Figure 3 - 4

3.2 Analysis of Computational Results

We now analyze the output of our extensive computational work. The results of this analysis are listed below.

1. We first notice that the in-track errors surpass in magnitude the cross-track errors. Our analysis will, therefore, address mainly the in-track errors. Then we also notice a remarkable difference between the two types of errors: the in-track errors exhibit a secular-like effect to which periodic effects are super-imposed while the cross-track errors are always of a periodic nature. The periodic effect is generally the result of short and long periodic effects. The short periodic effect can be recognized in all diagrams. Its period is related to the period of the satellite orbital revolution (in our case 100 minutes). Searching for long periodic effects, the period of which is nearly equal to an integral fraction of a day, is more difficult because they may be superimposed to other periodic effects, thus the behavior of the curve becomes distorted. Inspecting a selection of diagrams we can, however, clearly recognize the 12 hour, 8 hour, 6 hour periods, and so on. This is, respectively, the case of the diagram for $S_{7,2}$ (Figure 3-5), for $S_{4,3}$ (Figure 3-6), for $C_{6,4}$ (Figure 3-7), and others. Sometimes the in-track effect is a concealed or distorted long periodic effect, although its existence can be explained by theoretical consideration.

2. The absolute value of the in-track error can grow after 900 minutes (about 9 revolutions) to more than 3 km for the greatest of the sectorial coefficients $C_{2,2}$ (Figure 3-1). We have

M	ØMEGA	C ØMEGA	I	E	A
0.0000	0.0000	0.0000	45.00000	.00500000	7136.6535

RUN FØR S(7 ,2) = .0832
FACTØR USED IS 1.000000

(*) IN-TRACK
(+) PRINCIPAL NØRMAL CRØSS-TRACK
(⊙) BI-NØRMAL CRØSS-TRACK

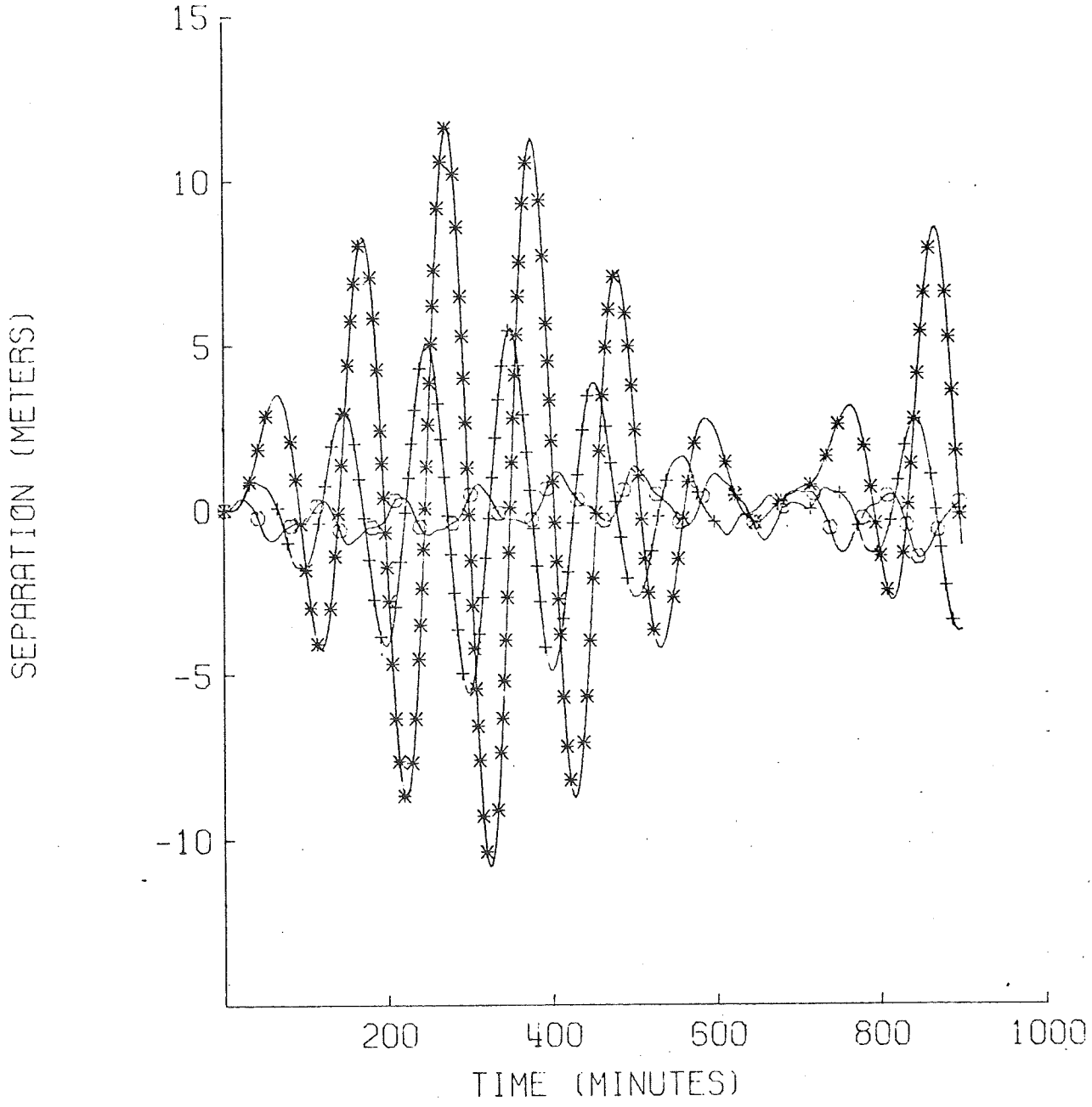

Figure 3-5

M	ØMEGA	C ØMEGA	I	E	A
0.0000	0.0000	0.0000	45.00000	.00500000	7136.6535

RUN FØR S(4 ,3) = -.2317
FACTØR USED IS 1.000000

(✳) IN-TRACK
(+) PRINCIPAL NØRMAL CRØSS-TRACK
(ⓘ) BI-NØRMAL CRØSS-TRACK

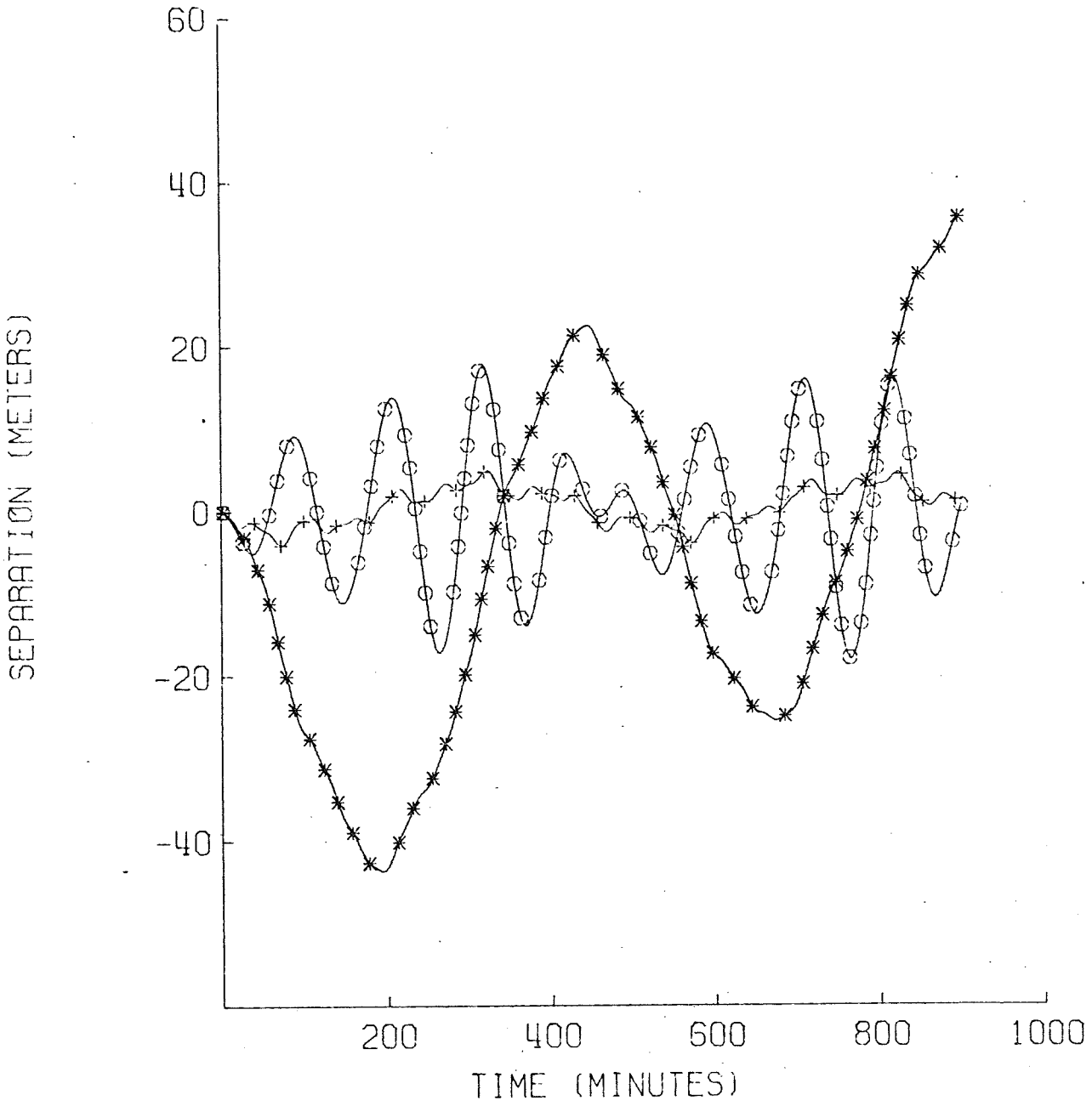

Figure 3-6

M	OMEGA	C OMEGA	I	E	A
0.0000	0.0000	0.0000	45.00000	.00500000	7136.6535

RUN FOR C(6 ,4) = -.0300
FACTOR USED IS 1.000000

(*) IN-TRACK
(+) PRINCIPAL NORMAL CROSS-TRACK
(⊙) BI-NORMAL CROSS-TRACK

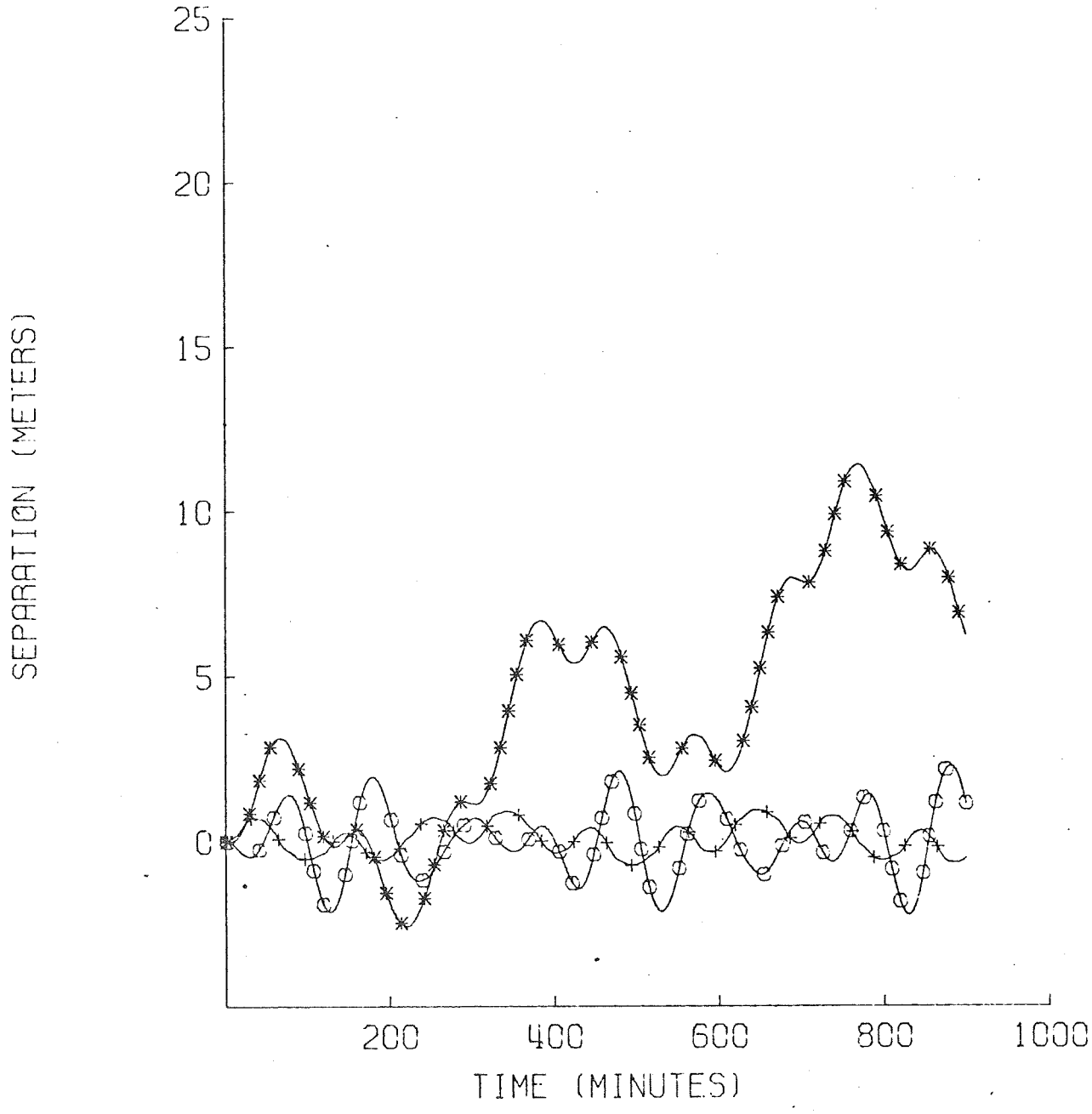

Figure 3-7

already seen that for an uncertainty equal to 2.23% of the magnitude of this coefficient the in-track error becomes 80 meters. This implies that this coefficient should be better determined than it is at the present time if we want to reduce the in-track error within the range (0, 10) meters. All other tesseral and sectorial coefficients induce smaller in-track errors. By increasing the order of the model the requirement on the accuracy becomes consequently less critical. For all the coefficients between (8, 0) and (14, 14), the magnitude of which is preponderantly within the range $(10^{-8}, 10^{-7})$, the in-track error reduces to 20, 10 and less than 10 meters after the same span of 900 minutes.

3. In regard to the zonal harmonic coefficients ($n \neq 0$, $m = 0$) the induced in track error, as expected, is either of secular or periodic nature according to n even or odd, respectively.

4. The sectorial harmonic coefficients ($n = m$) always induce secular like effects. An example is given in the diagram for $S_{12,12}$ (Figure 3-8). We have experimentally found that for the orbit under investigation, the ratio $\left| \frac{\Delta S}{J_{n,m}} \right|$, where ΔS indicates the in-track error at $t = t_0 + 900$ minutes, is approximately close to 10^{-3} for all sectorial coefficients except for $C_{13,13}$ and $S_{13,13}$ in which cases this ratio becomes about 2.6×10^{-3}.

5. Among the tesseral harmonic coefficients ($n \neq m$) when n is a multiple of m, we can recognize a different behavior in the in-track error induced by a C or S coefficient. Precisely, a C coefficient induces a markedly periodic effect to which a sensible secular-like effect is superimposed. An S coefficient induces instead a secular-like effect to which

M	ØMEGA	C ØMEGA	I	E	A
0.0000	0.0000	0.0000	45.00000	.00500000	7136.6535

RUN FØR S(12 , 12) = -.0332
FACTØR USED IS 1.000000

(*) IN-TRACK
(+) PRINCIPAL NØRMAL CRØSS-TRACK
(⊕) BI-NØRMAL CRØSS-TRACK

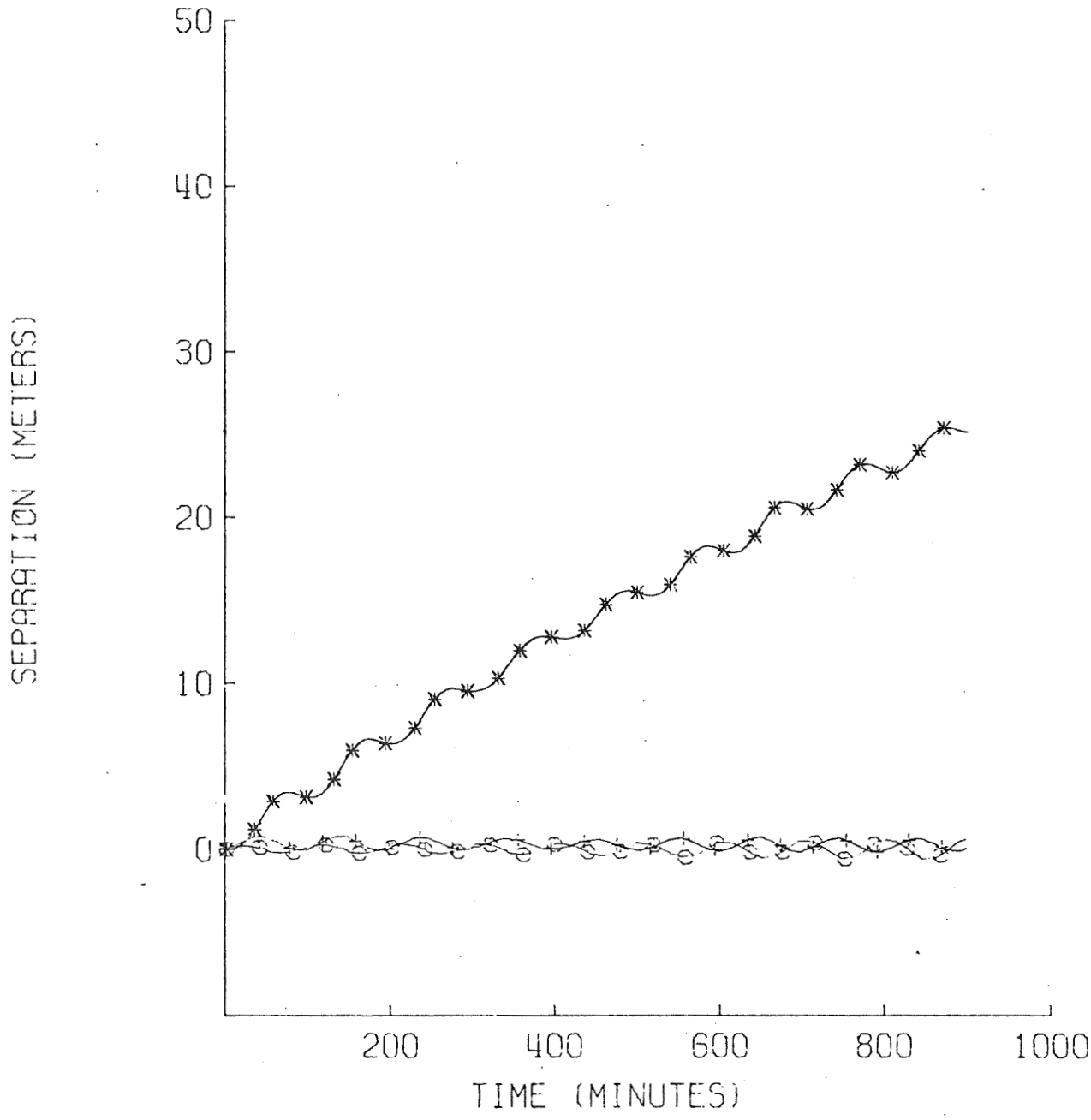

Figure 3-8

an oscillation of small amplitude is superimposed. Typical examples for both cases are shown in the diagrams for $C_{9,3}$ (Figure 3-9) and $S_{12,6}$ (Figure 3-10) respectively.

6. There is no possibility of predicting the sign of the in-track error induced by many coefficients at the end of the interval integration. This sign changes erratically although we can say that it depends on many factors,

   - o the sign of the harmonic coefficient under consideration
   - o whether n and m are both even or odd or one is even and the other is odd
   - o the position of the earth with respect to the position of the satellite in its orbit at time t because of the presence of the functions $\cos(m\lambda)$ or $\sin(m\lambda)$ in the integrand (λ is the longitude of the satellite.).

   Despite this lack of information, in any actual computation, it turns out that a sort of compensation among positive and negative in-track errors takes place when global effects are computed. This will be discussed next.

7. From the diagram (Figure 3-11) showing the averaged absolute value of the in-track error for all the coefficients of the geopotential whose magnitude is less than 10^{-7} we recognize that most of the coefficients induce errors less than 20 meters. In this diagram abscissas and ordinates are in logarithmic scales. The abscissas have been computed by:

   $x = \log_{10} \left| 10^{10} J_{n,m} \right|$, where $J_{n,m}$ is either a C or an S coefficient.

   The ordinates are expressed in meters. The numbers between the dashed lines indicate the percentage of the coefficients.

M	ØMEGA	C ØMEGA	I	E	A
0.0000	0.0000	0.0000	45.00000	.00500000	7136.6535

RUN FØR C(9 ,3) = -.0575
FACTØR USED IS 1.000000

(*) IN-TRACK
(+) PRINCIPAL NØRMAL CRØSS-TRACK
(⊙) BI-NØRMAL CRØSS-TRACK

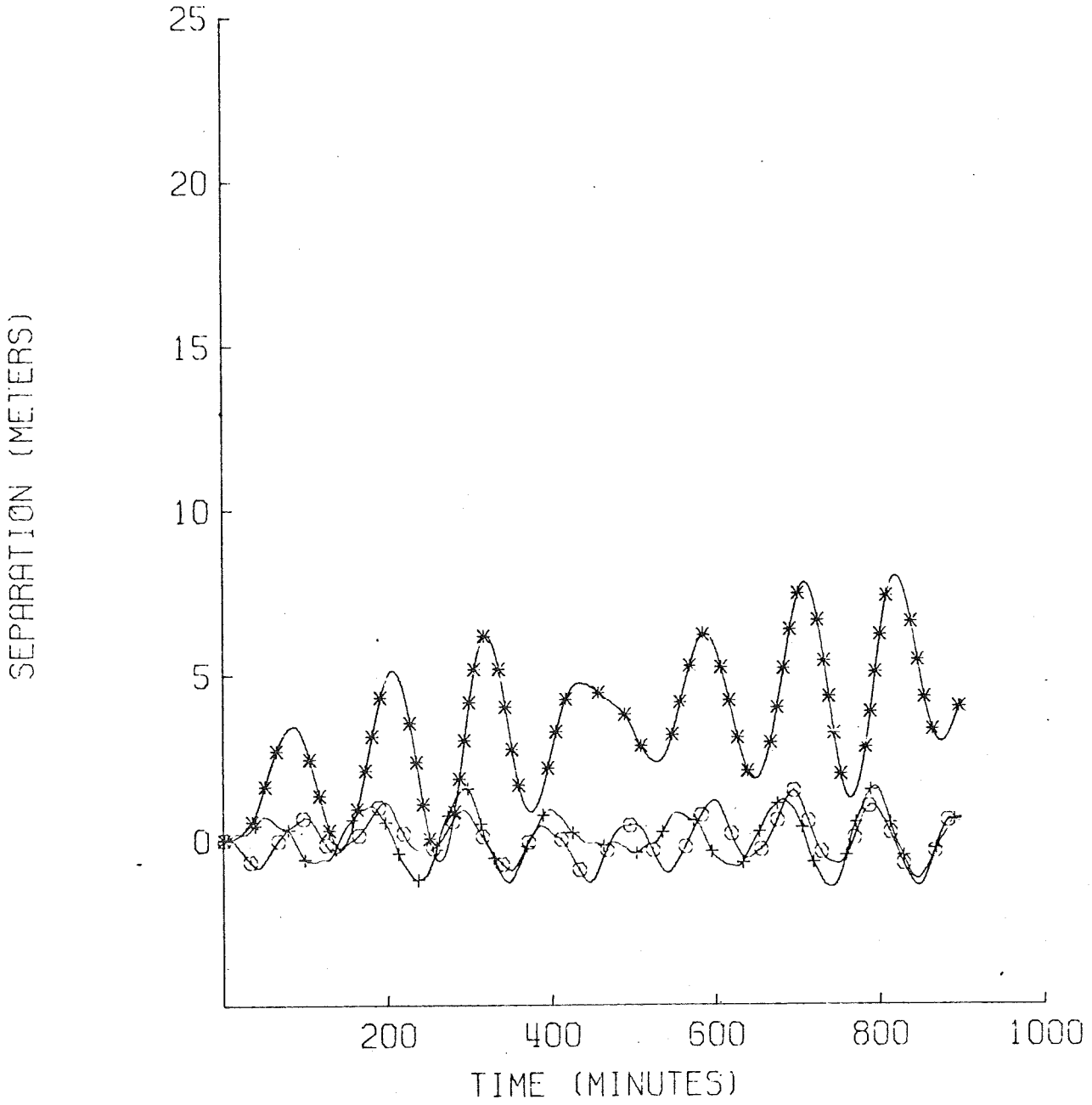

Figure 3 - 9

M	ØMEGA	C ØMEGA	I	E	A
0.0000	0.0000	0.0000	45.00000	.00500000	7136.6535

RUN FØR C(12 , 6) = .0354
FACTØR USED IS 1.000000

(✳) IN-TRACK
(+) PRINCIPAL NØRMAL CRØSS-TRACK
(⊙) BI-NØRMAL CRØSS-TRACK

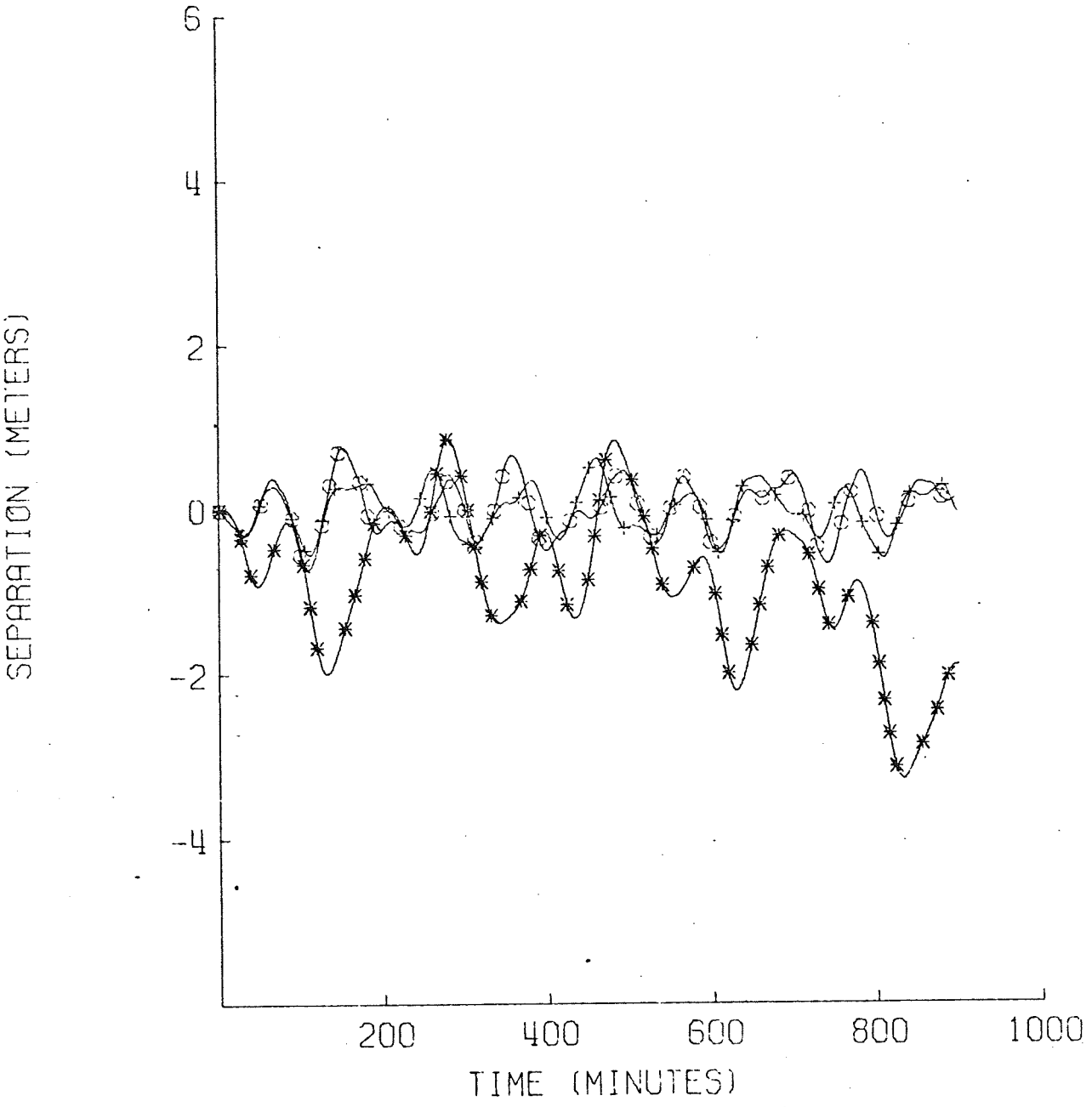

Figure 3 - 10

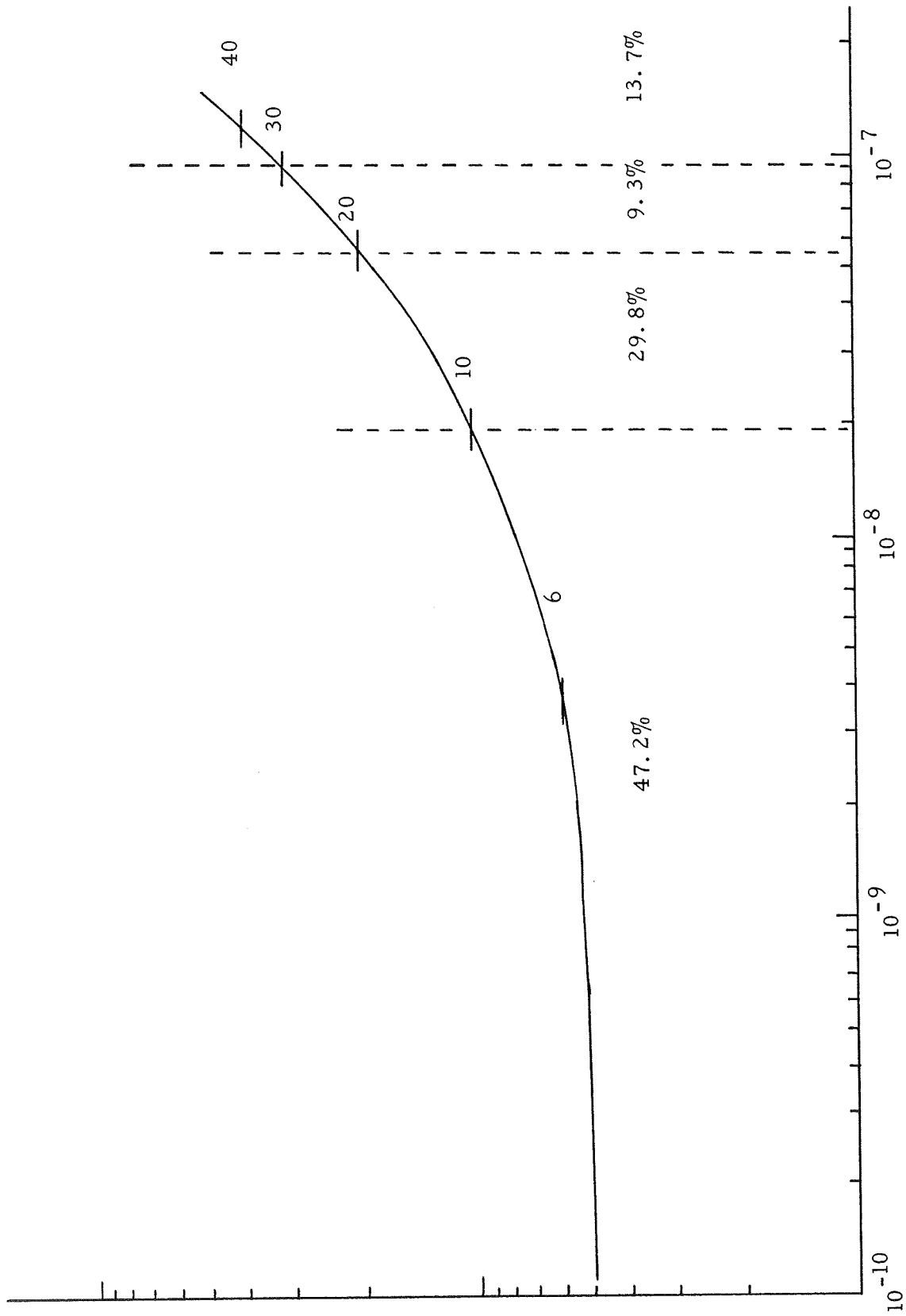
Averaged Absolute Values of the In-track Errors
Produced by Coefficients of Order less than 10^{-7}
100
10
1
10^{-10}
10^{-9}
10^{-8}
10^{-7}
40
30
20
10
6
47.2%
29.8%
9.3%
13.7%

Figure 3-11

The coefficients contributing to the far-right portion of the curve ($x > 3$, that is $|J_{n,m}| > 10^{-7}$) are $C_{9,1}$, $C_{9,8}$ $C_{10,9}$, $C_{12,3}$, $C_{14,5}$, and $S_{8,2}$, $S_{8,6}$, $S_{8,8}$, $S_{10,3}$, $S_{10,8}$, $S_{11,7}$, $S_{12,5}$. Almost all belong to the category of poorly determined coefficients, ($0.25 |J_{n,m}| < \sigma_{n,m} < |J_{n,m}|$). Among these coefficients $C_{9,8}$ and $S_{8,2}$ are the greatest in absolute value.

8. An interesting result is shown in the two diagrams (Figures 3-12 and 3-13) which have been obtained from Figure 3-11 by separating the positive from the negative in-track errors. The curve of the first diagram is approximately represented by the equation:

$$y^{(+)} = 6.61\, e^{12.9x}$$

while the second curve is represented by the equation:

$$y^{(-)} = -6.47\, e^{14.7x} \quad .$$

The numerical factors and exponents in both equations have been obtained by least square curve fitting among given data points. Composing the two curves into a single curve:

$$y = y^{(+)} + y^{(-)}$$

it is remarkable to find that up to $x = 3$ it is $|y| < 10$ meters while for $x > 3$, $|y| > 10$ meters.
The curve $y = y^{(+)} + y^{(-)}$ has been plotted in the diagram titled "Composition between positive and negative errors", (Figure 3-14). This curve gives graphical evidence of the compensation which takes place among averaged positive and negative errors.

Figure 3-12

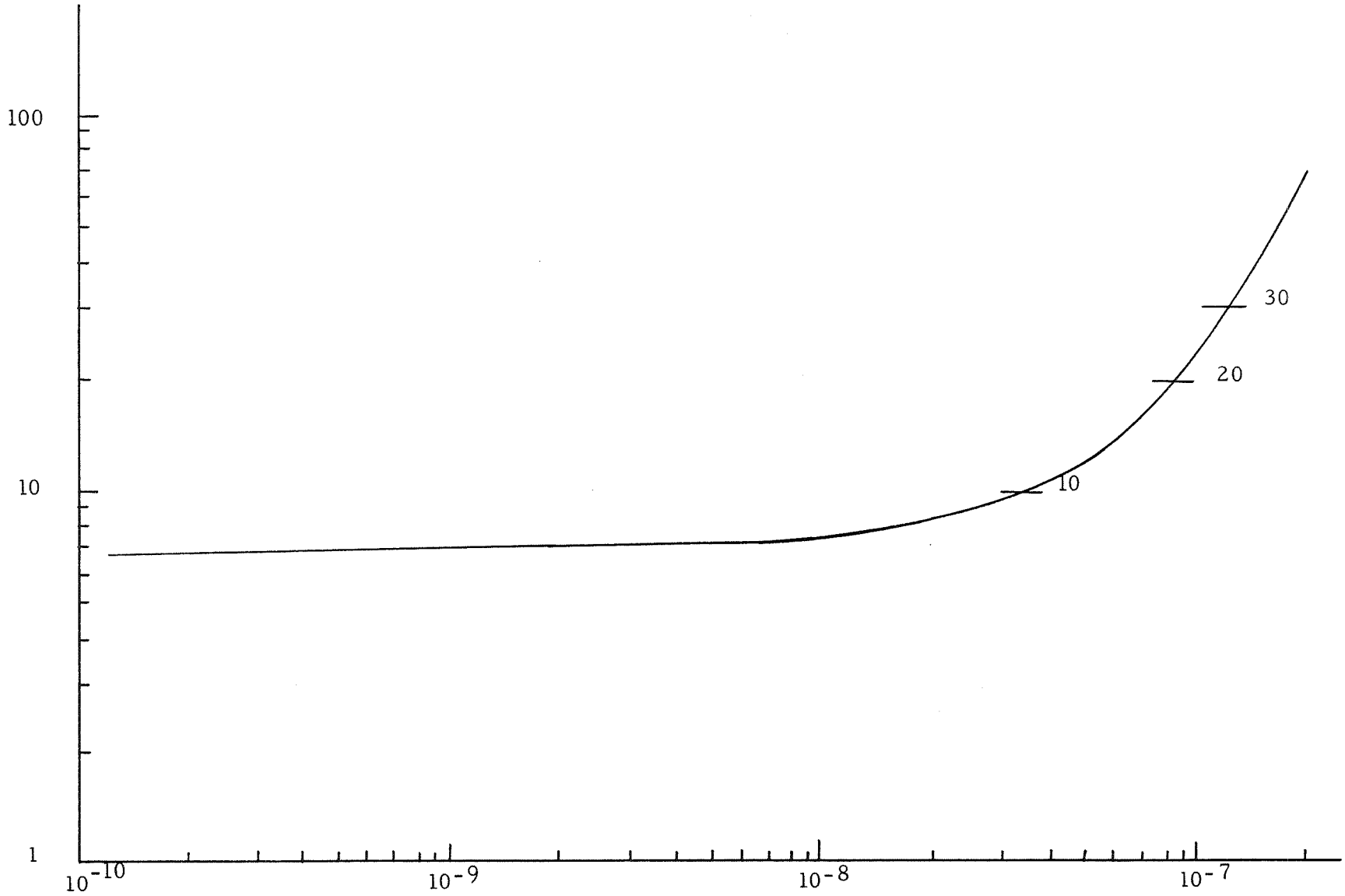

Averaged positive values of the in-track errors produced by coefficients of order less than 10^{-7}

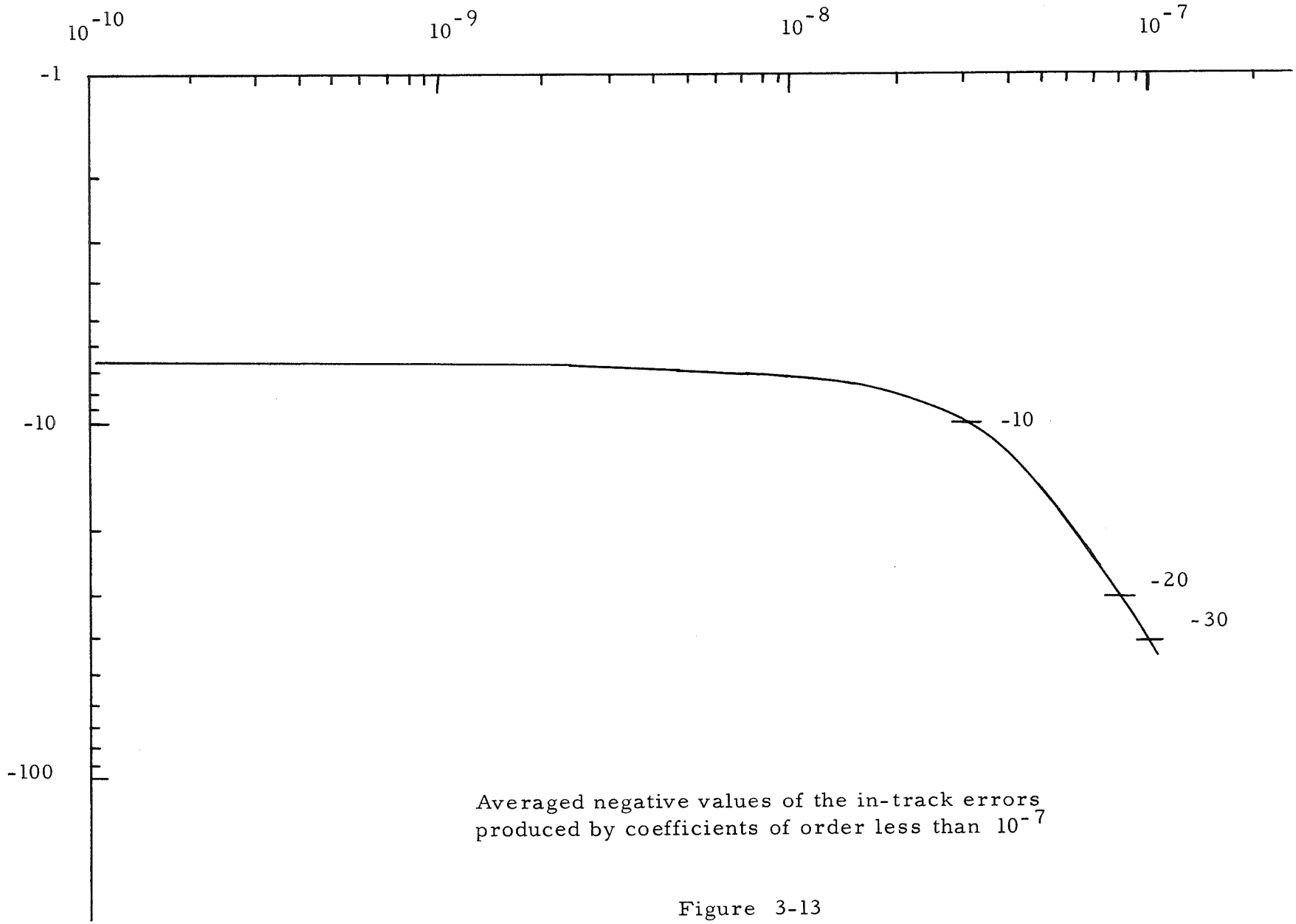

Averaged negative values of the in-track errors produced by coefficients of order less than 10^{-7}

Figure 3-13

Compensation between positive and negative errors ($y = y^{(+)} + y^{(-)}$)

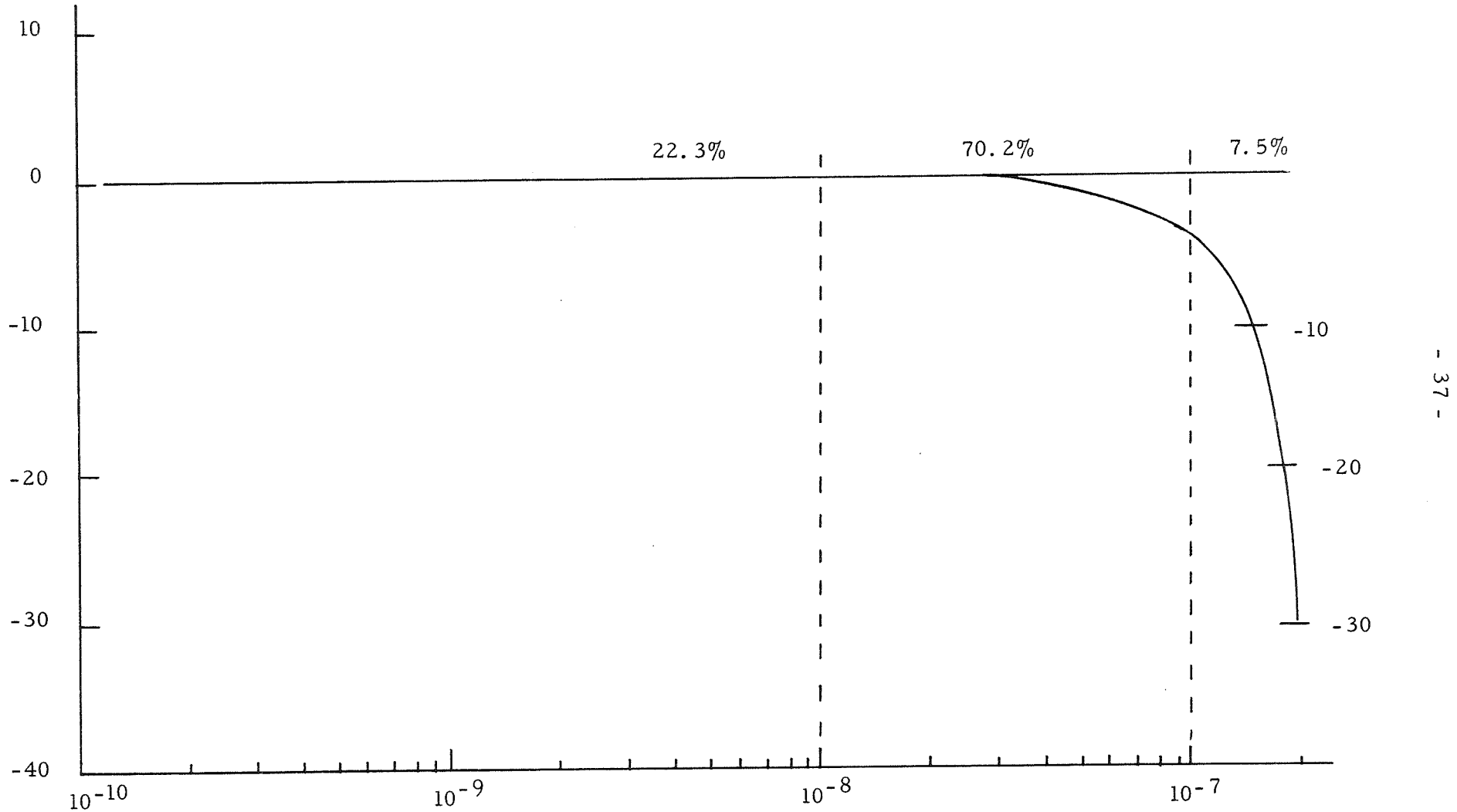

Figure 3-14

9. A more striking evidence of this compensation can be given if we derive the curve representing the growth of the global effect (Figure 3-15) when all coefficients are taken into account simultaneously. The growth of the error is given for models of increasing order, precisely, fourth, sixth, eighth order and so on. Our computations indicate that there is no perceptive difference, qualitatively and quantitatively, to be noticed among curves for models of order greater than the 8th order. The curves for the 10th and higher order models thus have not been plotted simply because they coincide with that of the 8th order model. We may conclusively say that the said compensation tends to be stabilized when we reach the 8th order model It is worth noticing that along with the plotting of the curves under consideration, we have had the opportunity to give a numerical proof of the validity of the additive property of small perturbations which has been quoted very often in this paper. The ordinates of these curves have in fact been checked at selected abcissas against the sum of the ordinates of the single components evaluated at the same abscissas and they have been found to be in agreement to within a few meters.

Our discussion and analysis enable us to make the following statements:

a) Effect of the uncertainty in a single term

The effect of an uncertainty in a single geopotential coefficient is small and is proportional to the effect produced by the coefficient itself. This is true as long as the uncertainty is not larger than the magnitude of the corresponding coefficient. For high order

IN-TRACK COMPONENT FOR MODELS OF DIFFERENT ORDER

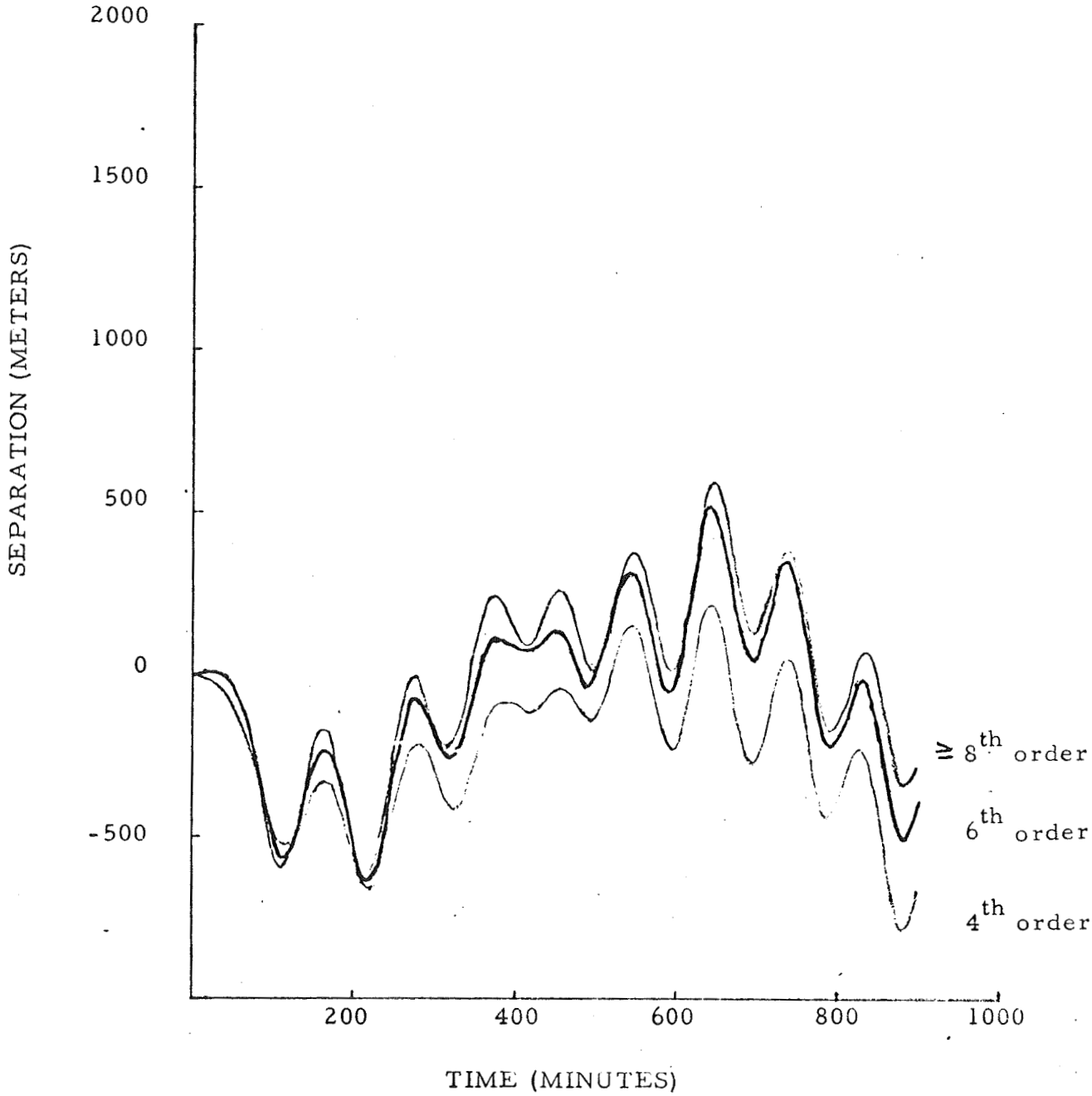

Figure 3-15

terms, however, greater uncertainties are not critical.

b) Global effect

Considered globally, the effects of the uncertainties in the coefficients are similar to the effects due to the coefficients themselves. There is an analogous phenomenon of global compensation for the uncertainties as that described above in 9) for the coefficients, hence their global effect on the prediction remains negligible.

c) Sufficiency of a consistent set of correlated coefficients

Except for a few well determined geopotential coefficients, the present knowledge of the external fine structure of the gravitational potential is not reliable. The standard errors associated with these coefficients are very often too large. Consequently, the knowledge of the corresponding coefficients remains fairly uncertain. Notwithstanding several investigators have derived consistent but correlated sets of coefficients from either satellite geodesy or gravimetric ground measurements, and even from a combination of both techniques. As a result, a potential model based upon any of these consistent sets is capable of providing a motion description which satisfactorily fits the satellite positions derived from observations. This fit may be extended to a variable interval of time which, according to the size and shape of the orbit - and whether other perturbing effects can or cannot be

neglected - may cover from a few to many revolutions of the satellite around the earth.

d) Feasibility of obtaining an accuracy within ± 10 m. Using a selected consistent set of geopotential coefficients (we used Rapp's set), our numerical analysis shows that the prediction of satellites' positions within 10 meters during 12 hours seems to be feasible using a model that includes terms up to the 8th order and selected terms of higher order. This happens because of the said global compensation which takes place among the positive and negative errors. This global compensation becomes more evident by increasing the order of the model. The selection of the selected terms which contribute to the achievement of the 10 meters accuracy will require an additional close scrutiny of our numerical investigation.

4. FUTURE EFFORT

During the first phase of this study, a base orbit was selected and studied extensively. In the future, the results obtained using this orbit will be extended to other orbits in the range of interest to parameterize the results with respect to orbital period, inclination, and eccentricity. In carrying out this additional effort, selected harmonic coefficients will be investigated and the functional variation of a coefficient with respect to some parameter will be determined. These functional variations will be utilized to investigate the remainder of the coefficients, but will include a system of checks to assure that the technique provides definitive results.

Resonant orbits will be investigated with respect to the associated coefficients to avoid their contaminating the general results. For the resonant effects whose period exceeds one day, the analysis should provide the appearance of a long periodic or secular effect since the study will be limited to the 700 - 900 minute period that was previously adopted.

The first step in the future effort will be to parameterize results with respect to inclination for the 100 minute orbit. Following this, the period will be increased in steps of 5 minutes and the eccentricity will be varied such that altitude does not fall below approximately 700 km. The 700 km limitation is being set on the basis of atmospheric effects at the present time.

The study may also be extended to lower altitudes without the inclusion of air drag to obtain accurate estimates of the geopotential perturbations due to uncertainties in the coefficients. These uncertainties will be compared with the effects of uncertainties in atmospheric perturbations to provide a quantitative measure in the region where geopotential studies are of questionable value because of atmospheric effects.

The results of the parameterization studies will then be used in an evaluation of the geopotential models required to obtain specified prediction accuracies over the period of interest. In addition, procedures will be outlined whereby models may be modified through the inclusion of improved values for selected coefficients based on independent results by various researchers.

5. REFERENCES

Izsak, I, "A new Determination of Non-Zonal Harmonics by Satellites", in Trajectories of Artificial Celestial Bodies as Determined from Observations, Springer Verlag, Berlin, 1966.

Kaula, W. M., "Theory of Satellite Geodesy", Blaisdell Publishing Company, Waltham, Massachusetts, 1966.

Rapp, R. H., "The Geopotential to (14, 14) from a Combination of Satellite and Gravimetric Data", Presented at XIV General Assembly International Union of Geodesy and Geophysics, September 25 - October 7, 1967.

Izsak, I, "Tesseral Harmonics of the Geopotential and Correction to Station Coordinates", Journal of Geophysical Research, vol. 69, p. 2621, 1964.

Strange, W. et al, "Requirements for Resonant Satellites for Gravimetric Satellite Geodesy", Report by Geonautics, Inc., 803 West Broad Street, Falls Church, Virginia, 1967.

- APPENDIX A -

THE EARTH's GEOPOTENTIAL

The gravitational potential U outside of the earth is generally represented by the potential of a spherically homogeneous body U_o plus a disturbing potential R.

$$U = U_o + R = \frac{GM}{r} + R$$

Since the earth is nearly spherical and hence $R << U_o$, the potential U can be approximated by an expansion in spherical harmonics. The standard form of the expansion adopted by the IAU at the meeting at Berkeley in 1962 is given by:

$$U = \frac{\mu}{r}\left[1 + \sum_{n=1}^{\infty}\sum_{m=0}^{n}\left(\frac{a_e}{r}\right)^n P_n^m(\sin\beta)\left(C_{n,m}\cos m\lambda + S_{n,m}\sin m\lambda\right)\right]$$

where

$\mu = GM$ = The gravitational parameter of the earth
r = The geocentric radius to the point of interest
a_e = The equatorial radius of the earth
$C_{n,m}, S_{n,m}$ = Harmonic coefficient in the expansion
λ = Longitude East of the Greenwich meridian
β = Geocentric latitude
$P_n^m(\sin\beta)$ = Legendre polynomials and associated functions.

It is assumed that the origin of coordinates is at the mass center of the earth, then the n = 1 terms in U are zero by definition.

The physical representation of the equation for U is to assume that the gravitational field can be represented by a surface distribution

of mass. The first part μ/r represents a spherically symmetric distribution of mass and the remainder defines superimposed regions of mass excess or deficiency. These latter regions are bounded by the zeros in the harmonic functions $\cos m \lambda$, $\sin m \lambda$ and the Legendre polynomials. For a given n, there are n-m zeroes in latitude and 2m zeroes in longitude as shown in typical examples below:

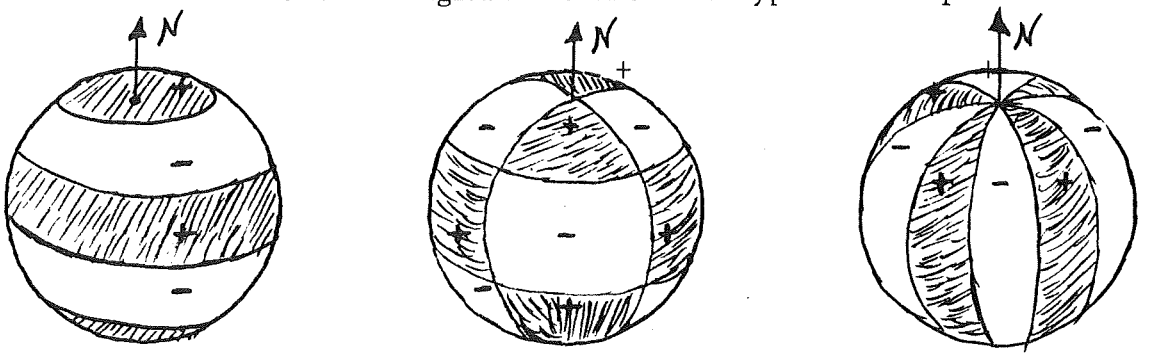

n=4 m=0	n=4 m=2	n=4 m=4
no zeros in longitude 4 zeros in latitude zonal term	4 zeros in longitude 2 zeros in latitude tesseral term	8 zeros in longitude no zeros in latitude sectorial term

Because of the way the earth is mathematically represented by a tessera (checkerboard) the terms are in general called tesseral, although the two extreme cases are generally called zonal and sectorial since the crossing lines forming the tessera are not existant.

The value of the mass excess or deficiency is given by the value of the coefficients $C_{n,m}$, $S_{n,m}$ which give the amplitudes of the harmonic functions $\cos m \lambda$ and $\sin m \lambda$. The gravitational field could be represented to any desired degree of accuracy if all the C's and S's were known. Since they are not, the degree to which it can be represented from an orbit prediction accuracy requirement is open to question and defines the present problem.